Nuclear Instruments and Methods in Physics Research B 269 (2011) 2168–2174

Contents lists available at ScienceDirect

Nuclear Instruments and Methods in Physics Research B

journal homepage: www.elsevier.com/locate/nimb

The Singapore high resolution single cell imaging facility

Frank Watt *, Xiao Chen, Armin Baysic De Vera, Chammika N.B. Udalagama, M. Ren, Jeroen A van Kan, Andrew A Bettiol

Centre for Ion Beam Applications, Dept. of Physics, National University of Singapore, Science Drive 3, Singapore 117542, Singapore

ARTICLE INFO

Article history:
Available online 26 February 2011

Keywords:
Nano-imaging
Nano-STIM
STIM
Scanning transmission ion microscopy
Single cell imaging
Proton induced fluorescence microscopy

ABSTRACT

The Centre for Ion Beam Applications, National University of Singapore has recently expanded from three state-of-the-art beam lines to five. Two new beam lines have been constructed: A second generation proton beam writing line, and a high resolution single cell imaging facility. Both systems feature high demagnification lens systems based on compact Oxford Microbeams OM52 lenses, coupled with reduced lens/image distances.

The single cell imaging facility is designed around OM52 compact lenses capable of operating in a variety of high demagnification configurations including the spaced Oxford triplet and the double crossover Russian quadruplet. The new facility has design specifications aimed at spatial resolutions below 50 nm, with a variety of techniques including STIM, secondary electron and fluorescence imaging, and an in-built optical and fluorescence microscope for sample imaging, identification and positioning.

Preliminary tests using the single space Oxford triplet configuration have indicated a beam spot size of 31×39 nm in the horizontal and vertical directions respectively, at beam currents of ~10,000 protons per second. However, a weakness in the specifications of the electrostatic scanning system has been identified, and a more stable scanning system needs to be implemented before we can fully realize the optimum performance. A single whole fibroblast cell has been scanned using 1.5 MeV protons, and a median fit to the proton transmission energy loss data has shown that proton STIM gives excellent details of the cell structure despite the relatively poor contrast of proton STIM compared with alpha STIM.

1. Introduction

The Centre for Ion Beam Applications, National University of Singapore, has been substantially expanded over the past 2 years, and now has five state-of-the-art beam lines attached to a 3.5 MV high brightness HVEE (High Voltage Engineering Europa) Singletron™ ion accelerator. The beam lines are being used in a broad range of research activities, from analysis and characterisation of biomedical samples and advanced materials using nuclear microscopy/ion beam analysis (IBA), to the manufacture of devices and structures in the fields of microfluidics, microphotonics, microengineering, and biochip fabrication using proton beam writing and ion beam modification of materials.

In this paper we describe one of the two new beam lines; the high resolution single cell imaging facility. The justification for constructing this new facility is twofold: (a) there is an increasing demand for high resolution techniques that can image biological cells in novel ways, applicable for example to cell biology, biomedicine and targeted delivery of pharmaceuticals, and (b) recent work by the CIBA group [1] has indicated that not only does a finely focused beam of MeV protons maintain resolution as it passes through a whole biological cell, but the induced secondary electrons are in general short range, and have a lateral span of only a few nanometres. This raises the interesting possibility that if we can focus the proton beam to spot sizes below 10 nm, then not only will we be able to image the interior structure of cells with high resolution using scanning transmission ion microscopy (STIM), but proton induced fluorescence (PIF) microscopy can also be realised at resolutions below 10 nm.

In previous experimental work, STIM and PIF imaging at sub-100 nm resolutions has been demonstrated. MCF-7 (American Type Culture Collection [ATCC]) breast cancer cells have been imaged using alpha STIM at 50 nm resolutions [2], and murine RAW 264.7 macrophages stained with Mitotracker Red CMX-Ros (Invitrogen) have been imaged using proton induced fluorescence at around 60 nm spatial resolutions (to be published).

2. Description of the high resolution single cell imaging facility

The design specifications of the new facility are as follows: (a) Sub 50 nm resolutions (at low proton current), featuring high demagnification imaging and short lens-image distance, (b) the capability of STIM, secondary electron and fluorescence imaging,

* Corresponding author. Tel.: +65 65162815.
E-mail address: phywattf@nus.edu.sg (F. Watt).

0168-583X/$ - see front matter © 2011 Elsevier B.V. All rights reserved.
doi:10.1016/j.nimb.2011.02.028

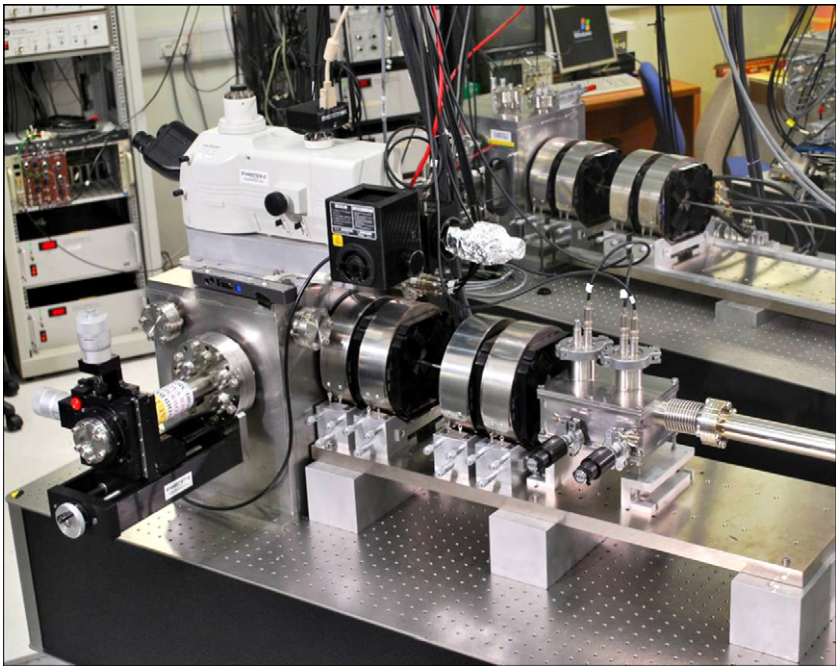

Fig. 1. Layout of the single cell imaging facility, showing from right to left: the electrostatic scan module, the 4 OM52 quadrupole lenses, and the target chamber (with the side mounted *XYZ* stage and the top mounted microscope).

(c) the capability of PIXE and RBS, although it must be noted that since these techniques require at least 100 pA proton current, sub-100 nm resolutions are unlikely to be achieved using conventional ion accelerator systems, (d) in-built optical and fluorescent microscope for sample imaging, identification and positioning, (e) accurate and stable sample manipulation using piezoelectric drivers, and (f) up to 2048 × 2048 pixel imaging using IonDaq [3].

The beam optical system follows the normal layout of microprobe formation, that of a demagnified image of the beam passing through an object aperture. In our case we use differential micrometer controlled beam apertures (Oxford Microbeams Ltd. OM10) both as object apertures and also as downstream collimator slits to control beam aberrations. The layout of the cell imaging facility end stage is shown in Fig. 1, which indicates (i) the purpose built electrostatic scanning system, (ii) the lens system, made up of 4 compact OM52 quadrupole lenses, and (iii) the target chamber.

Proton beam scanning is achieved electrostatically, since hysteresis effects are in general less compared with magnetic scanning. A module containing *X* and *Y* parallel plates positioned just before the lens system is driven by 2 electrostatic amps (Trek high voltage amplifiers model 609E6) via IonDaq [3].

The lens configuration includes a space equal to 1 lens length (in this case 55 mm) between the 1st lens doublet and the second doublet. This enables the following lens configurations to be tested: The single spaced Oxford triplet (using lenses 2, 3 and 4), the double spaced Oxford triplet (using lenses 1, 3 and 4), and the single spaced Russian quadruplet. Note that since the conventional Russian quadruplet has relatively low demagnifications, we intend to use this type of configuration in a single-space double-crossover mode, which has greatly increased demagnifications in both the *X* and *Y* directions [4]. For this paper, we present only the preliminary results of the single spaced Oxford triplet. In table 1, the beam optics parameters of both the spaced triplet configuration used in the new beam line are compared with the beam optics of the existing proton beam writing line which has achieved spot sizes (low current) of 35 × 75 nm [5]. As expected,

Table 1
Beam characteristics of the new cell imaging line, compared with the existing proton beam writing line: Note that the increased demagnifications are accompanied by greatly increased spherical aberrations. Note also that the beam brightness is reduced compared with the values listed in [5], due to a change to the ion source electronic circuitry.

Beam optics parameters	Proton beam writing line [5]	Cell imaging line
Object aperture to lens distance	6.4 m	7.5 m
Beam focus to lens distance	7 cm	4 cm
X,*Y* demagnification	228, −60	472, −87
Object aperture (A_o) setting (Δx, Δy)	2 × 2 μm (approx)	15 × 3 μm (approx)
Collimator slit aperture (A_a) setting (Δx, Δy)	10 × 10 μm (approx)	10 × 10 μm (approx)
Beam brightness [$B = I/A_oA_aE/d^2$]	74 pA/μm^2.mr^2.MeV	∼20–30 pA/μm^2.mr^2.MeV
Chromatic aberration coefficients		
($x/\theta\delta$)	−385 μm/mr/%mom spread	−392 μm/mr/%mom spread
($y/\phi\delta$)	984 μm/mr/%mom spread	1029 μm/mr/%mom spread
Spherical aberration coefficients		
(x/θ^3)	2692 μm/mr^3	6258 μm/mr^3
($x/\theta\phi^2$)	1160 μm/mr^3	4167 μm/mr^3
(y/ϕ^3)	−13,620 μm/mr^3	−12,380 μm/mr^3
($y/\theta^2\phi$)	−4447 μm/mr^3	−22,550 μm/mr^3
Calculated geometric beam		
Spot size (x,y)	10×40 nm (nominal)	30 × 35 nm (nominal)

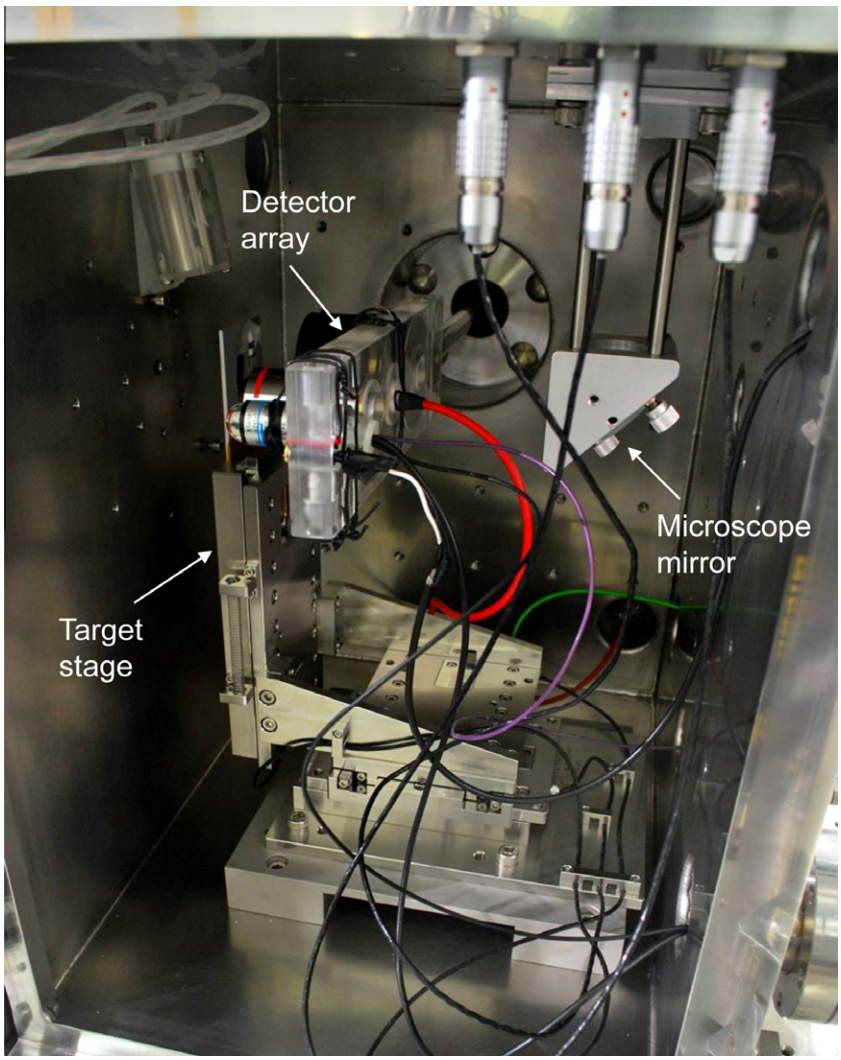

Fig. 2. Layout of the inside of the target chamber, showing the XYZ target stage, the detector array (which includes a 5× and 15× objective), and the mirror which transfers the target image into the top mounted microscope.

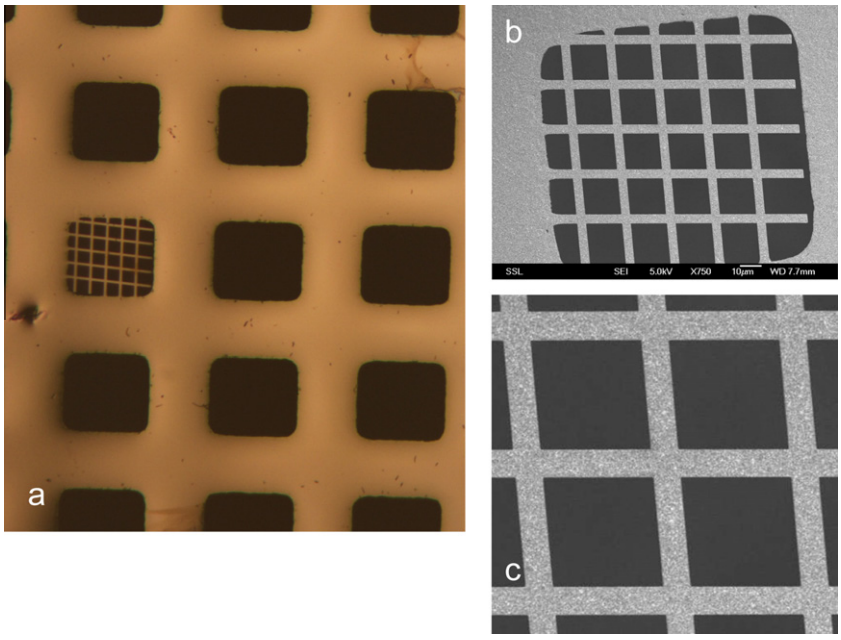

Fig. 3. (a) Optical image showing the calibration grid on the left hand side, (b) SEM image of the grid (low demagnification) and (c) SEM image of the grid (high demagnification).

the increased demagnification of the single spaced triplet is counterbalanced by increased aberrations, particularly spherical aberrations.

The inside of the target chamber is shown in Fig. 2. The chamber houses a piezoelectric *XYZ* positioning stage (PI N-310K059) controlled by the stage controller: E-861 NEXACT®, and is capable of 25 mm movement in each of the *XYZ* directions. The positioning stage holds the samples, which also includes a quartz target for optical focusing down to the micron level, and a calibrated grid for fine focusing. Detectors, including a pin diode STIM detector (Hamamatsu S1223), a conventional surface barrier RBS detector, a Hamamatsu photomultiplier (model PMT R7401P), and 2 objective lenses (5× and 15×) are mounted on a linear drive behind the target stage. The detectors and optical lenses are moved into place using a manual *XYZ* translator (model MTS MA1006) connected to the chamber side. A fixed mirror is positioned behind the moveable objective lenses to optically connect the sample image to the microscope (Nikon D-DIH Digital Imaging Head M including filter block and fluorescence illuminator) which is situated on top of the target chamber. The microscope also includes provision for sample illumination and fluorescence imaging.

3. Preliminary tests of the high resolution single cell imaging facility

Resolution tests of the new beam line (in the single spaced Oxford triplet mode) were undertaken using a calibration grid fabricated using proton beam writing in CIBA. Optical photographs and SEM scans of the Ni grid are shown in Fig. 3. The grid, which exhibits sharp sidewall edges has grid bar dimensions of 4 μm, and a nominal thickness of 2 μm. A 1.5 MeV proton beam was focused down using a combination of the quartz target and the grid, and on-axis STIM images were taken at 50 μm scan size and 10 μm scan size (Fig. 4a and b). The STIM images of the grid, taken at around 10,000 protons per second, were recorded at 1024 × 1024 pixels, defining pixel resolutions of 50 and 10 nm. Images of the grid are shown in Figs. 4a and b. A median fit of the data extracted from the list mode file showed greater contrast, allowing the tomography of the grid to be emphasised (Fig. 5). Fig. 6 shows horizontal and vertical lines profiles extracted from the grid image depicted in Fig. 5. These results indicate a beam spot size of 31 × 39 nm in the horizontal and vertical directions respectively, at beam currents

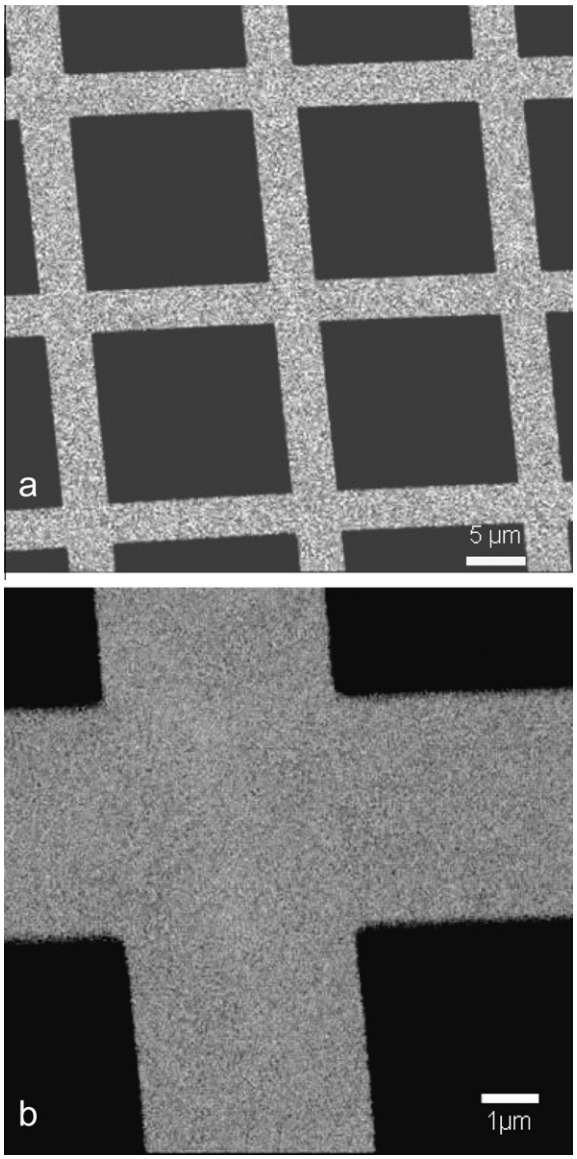

Fig. 4. (a) On-axis proton STIM scan of the calibration grid (scan size 50 μm) and (b) on-axis scan of the calibration grid (scan size 10 μm).

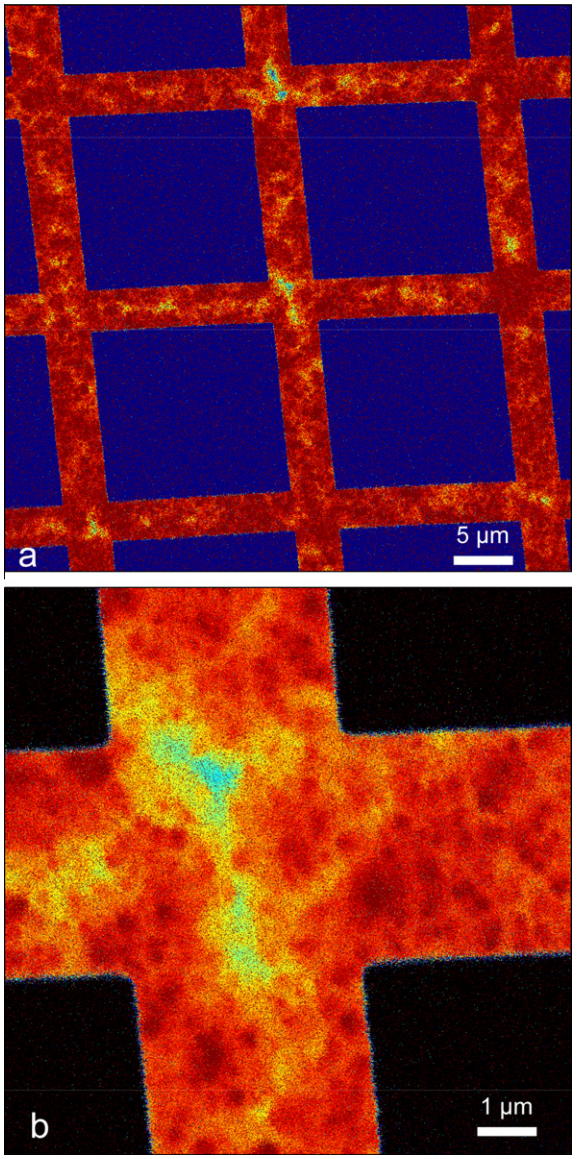

Fig. 5. (a) Median fit on-axis proton STIM scan of the calibration grid (scan size 50 μm) and (b) Median fit on-axis scan of the calibration grid (scan size 10 μm).

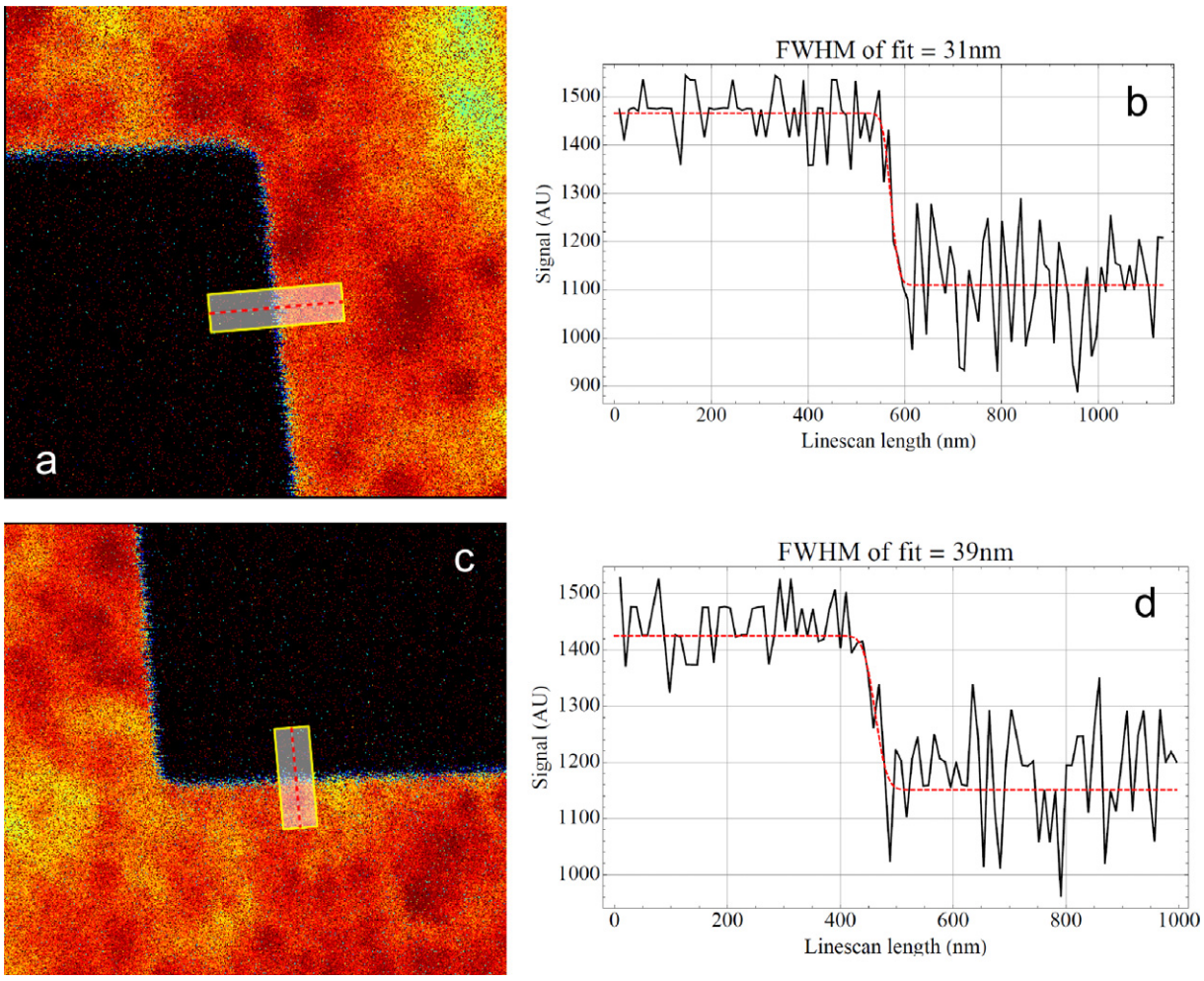

Fig. 6. Line profiles extracted from the grid image as shown in Fig. 5. (a) shows the area from which the data was extracted and (b) shows the line scan fit indicating a horizontal resolution of 31 nm. (c) shows the area from which the data was extracted and (d) shows the line scan fit indicating a vertical resolution of 39 nm. The fit was extracted using the formalism described in [6].

of around 10,000 protons per second. The fit to the line profiles are measured using the mathematical fitting routine described in [6].

Using the same beam current and the same beam optics settings as for the grid tests above, 1.5 MeV on-axis STIM images of a cell were also recorded. The cells (type MRC-5 human lung fibroblast) were grown and critical point dried on Si_3N_4 windows of dimensions 500×500 μm, with a thickness of 50 nm, using the protocol described in [2]. An optical image of the cells grown on the silicon nitride window is shown in Fig. 6a and the cell targeted for STIM mapping is shown in Fig. 6b. On-axis STIM images were recorded and are shown in Fig. 7a,b, and a median fit from the resulting list mode file is shown in Fig. 7c. It should be mentioned that proton STIM has a much less contrast than alpha STIM, since the energy loss of the 1.5 MeV proton beam passing through this cell (estimated at around 20–50 keV depending on cell thickness) is not much greater than the detector resolution. Nevertheless, the images indicate that reasonable detail can be observed within the cell, even when using proton STIM (Fig. 8).

4. Discussion and concluding remarks

A new facility has been constructed in CIBA, designed specifically for whole cell and tissue imaging. The design specifications include the provision of STIM, secondary electron and fluorescence imaging, spatial resolutions below 50 nm using high demagnification quadrupole lens systems, and an in-built optical and fluorescence microscope for sample imaging, identification and positioning.

Preliminary tests have shown that resolutions are consistent with sub 50 nm beam spot sizes. However, we have identified a weakness in the current electrostatic scanning system used in the preliminary tests. In order to achieve scan ranges of 200×200 μm down to 5×5 μm, with a pixel resolution of 10 nm at small scan sizes, the linearity of the scan driver and voltage amplifier should be consistent with 1 part in 2×10^4 step accuracy, and the noise levels should ideally be less than the step size. This is not the case at the moment. In addition, the nickel grid manufactured in CIBA using proton beam writing has a thickness of 2 μm. If the side wall is not vertical (and previous tests have shown that typically the side wall angle is around 89.4° to the vertical), then this will also add significantly to the spot size measurement. These factors will be addressed in the near future.

The development of proton induced fluorescence microscopy to its theoretical limit of sub 10 nm resolutions will represent a considerable advance on conventional fluorescence systems, since fluorescence or confocal microscopies are limited in resolving power to around 300 nm due to diffraction effects. Proton induced fluorescence microscopy will also have significant advances over the new super-resolution optical techniques specially developed to improve fluorescence imaging resolutions beyond optical diffraction limits. These new techniques include for example spatially

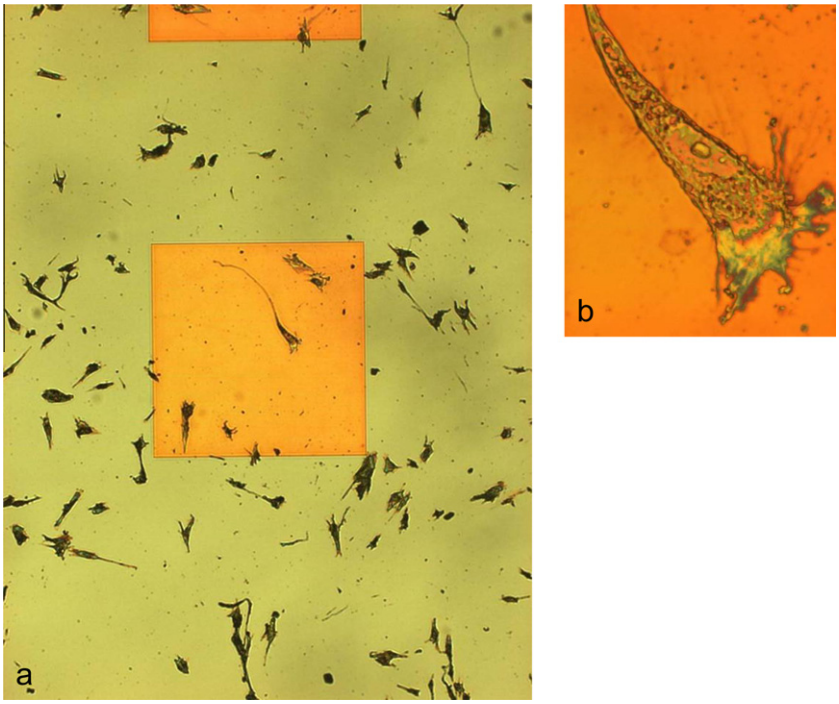

Fig. 7. (a) MRC-5 human lung fibroblast cells grown and critical point dried on Si_3N_4 windows: 500 × 500 μm in dimension, 50 nm in thickness, (b) an optical image of the cell chosen for scanning.

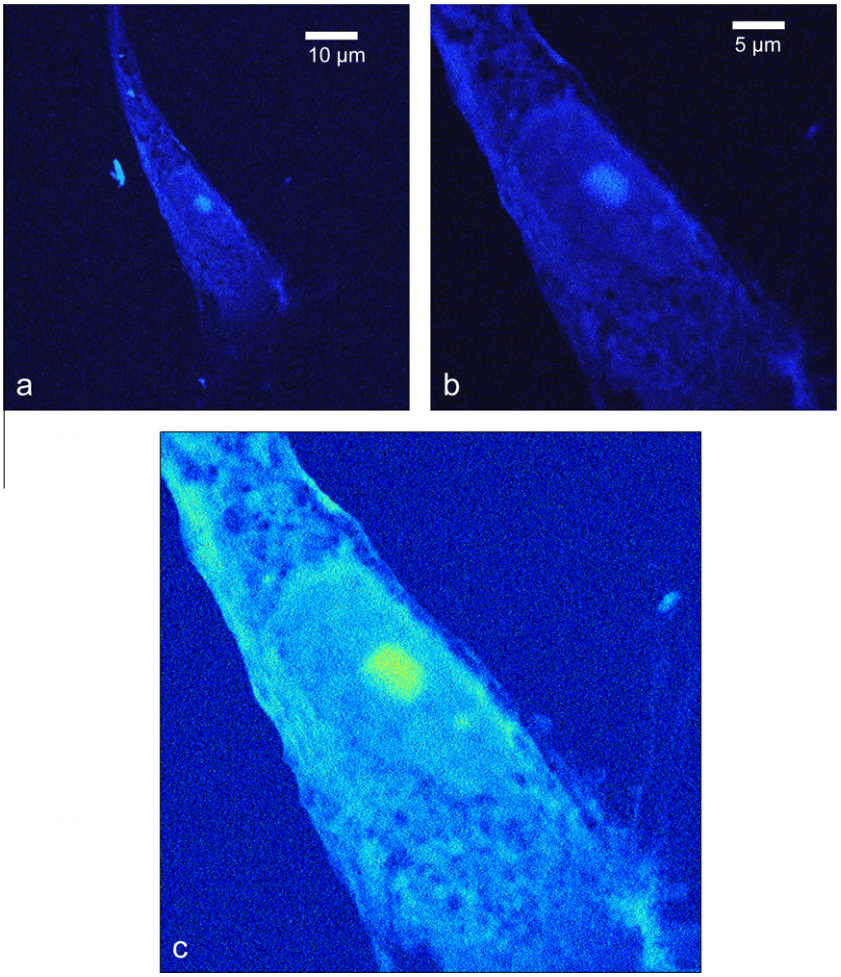

Fig. 8. (a) On-axis 1.5 MeV proton STIM: scan size (100 × 100 μ and (b) 50 × 50 μ (c) Median fit to the list mode data: scan size 50 × 50 μ.

modified illumination microscopy (SMI) [7], stimulated emission depletion (STED) [8], photo-activated localisation microscopy (PALM) [9–11] and nonlinear structured illumination [12,13]. A review of these recent biological imaging techniques, including a comparison of resolutions, can be found in [14].

Despite reaching a creditable proton beam resolution of around 30 nm, the main factor in the quest for sub 10 nm proton spot sizes is undoubtedly the ion source brightness. The RF source used in our accelerator has a brightness estimated at 20–30 pA/μm^2.mr^2.MeV, and the design has not changed significantly for 60 years. This is many orders of magnitude less than the corresponding electron sources. The design of a new ion source therefore is of paramount importance.

Acknowledgements

This study was supported by the Singapore Bioimaging Consortium (SBIC), ASTAR Grant number SBIC RP C-013/2007.

References

[1] C. Udalagama, A.A. Bettiol, F. Watt, Physical Review B 80 (2009) 224107.
[2] Ren Minqin, J.A. Van Kan, A.A. Bettiol, Lim Daina, Chan Yee Gek, Bay Boon Huat, H.J. Whitlow, T. Osipowicz, F. Watt, Nucl. Instr. Meth. B 260 (2007) 124–129.
[3] A.A. Bettiol, C. Udalagama, F. Watt, Nucl. Instr. Meth. B 267 (2009) 2069–2072.
[4] G.W. Grime, F. Watt, Beam Optics of Quadrupole Probe Forming Systems, Adam Hilger, Bristol, 1984. pp. 63.
[5] F. Watt, J.A. Van Kan, I. Rajta, A.A. Bettiol, T.F. Choo, M.B.H. Breese, T. Osipowicz, Nucl. Instr. Meth. B 210 (2003) 14–20.
[6] C.N.B. Udalagama, A.A. Bettiol, J.A. Van Kan, E.J. Teo, M.B.H. Breese, T. Osipowicz, F. Watt, Nucl. Instr. Meth. B 231 (2005) 389–393.
[7] D. Baddeley, C. Batram, Y. Weiland, C. Cremer, U.J. Birk, Nat. Protoc. 2 (10) (2007) 2640–2641.
[8] S.W. Hell, J. Wichmann, Opt. Lett. 19 (1994) 780–782.
[9] E. Betzig, G.H. Patterson, R. Sougrat, O.W. Lindwasser, S. Olenych, J.S. Bonifacino, M.W. Davidson, J. Lippincott-Schwartz, H.F. Hess, Science 313 (2006) 1642–1645.
[10] S.T. Hess, T.P. Girirajan, M.D. Mason, Biophys. J. 91 (2006) 4258–4272.
[11] M.J. Rust, M. Bates, X. Zhuang, Nat. Methods 3 (2006) 793–796.
[12] R. Heintzmann, T.M. Jovin, C.J. Cremer, Opt. Soc. Am. A. Opt. Image Sci. Vis. 19 (2002) 1599–1609.
[13] M.G.L. Gustafsson, Proc. Natl. Acad. Sci. USA 102 (2005) 13081–13086.
[14] M. Fernandez-Suarez, A.Y. Ting, Nat. Rev. Mol. Cell. Biol. 9 (2008) 929–943.